COBEM 2021 26th International Congress of Mechanical Engineering
ABCM Associação Brasileira de Engenharia e Ciências Mecânicas
November 22-26, 2021, Virtual Congress, Brazil

COB-2021-1795
PERCUSSION DRILLING AND SINGLE PULSE ABLATION ON AISI 1020 STEEL USING A 1064 µM NANOSECOND PULSED FIBER LASER

Santiago Javier Caraguay
Universidade Federal de Santa Catarina, Campus Reitor João David Ferreira Lima, Florianópolis – SC, 880400-900, Brazil.
Instituto Senai de Inovação em Sistemas de Manufatura e Processamento a Laser, Rua Arno Waldemar Dohler, Joinville – SC, 89218-153, Brazil.
scaraguayc@gmail.com

Thiago Soares Pereira
Instituto Senai de Inovação em Sistemas de Manufatura e Processamento a Laser
thiago.pereira@sc.senai.br

Fabio Antônio Xavier
Universidade Federal de Santa Catarina – UFSC
f.xavier@ufsc.br

Milton Pereira
Universidade Federal de Santa Catarina – UFSC
milton.pereira@ufsc.br

Abstract. *Laser drilling has benefits compared to other fabrication technologies because it is a non-contact process, with high accuracy, repeatability, and flexibility. Percussion drilling provides the advantage of higher drilling speed compared to trepanning and helical drilling. Holes prepared with this technique are usually used for surface conditioning prior to coating applications. Hole's diameter and depth are related to the processing parameters and obtaining a complete characterization of dimensions and geometrical aspects is needed to determine boundaries for further surface modification. In this context, the aim of this work is to produce holes by laser percussion drilling on AISI-1020 low carbon steel by nanosecond pulsed fiber laser at the fundamental wavelength of 1064 µm. By varying pulse energy, distance to focus, and number of pulses per spot, it was possible to fabricate holes of different diameters and depths. To better understand the laser-material interaction, the diameter regression method was used to evaluate the material ablation threshold. Single-pulse laser irradiations with incremental values of pulse energy were performed on the steel sample. Holes' diameters, holes' depths, and ablated craters diameters were characterized through optical microscopy. Scanning electron microscopy was used to characterize material removal after percussion drilling. Results showed an increase in hole diameter and hole depth with the increase of pulse energy and number of pulses, respectively. Resolidified material affects the geometrical characteristics of the fabricated holes. Ablated craters show a tendency of increased diameter values with the increase of laser energy.*

Keywords: *laser, percussion drilling, ablation threshold, regression method, material removal.*

1. INTRODUCTION

Corrosion of metals is a type of material degradation caused by chemical and electrochemical interactions between the metal and the environment. It is estimated that the annual cost of corrosion in the Oil and Gas Industry is in the order of 60 billion dollars (Papavinasam, 2013). In this industry, problems related to corrosion are critical considering that most equipment, pipeline, and structures used for production and transportation are made of carbon steel. Moreover, the environment is usually hypersaline and, therefore, very corrosive.

As one of the most applicable structure steels, largely used in non-critical components such as cold-headed bolts, shafts, frames, AISI 1020 steel is used in all industries as an affordable, easy-to-use material, with a great balance of performance. Thus, this material is often exposed to corrosive environments, requiring processes for corrosion mitigation in order to increase its life expectancy.

Protective painting is largely applied in order to protect metals against atmospheric corrosion. It consists of applying a protective coating on the surface to separate the metallic material from the corrosive environment. Mechanical interlocking is considered the most effective mechanism for coating resistance when exposed to corrosive environments

(Hagen *et. al.*, 2019). Mechanical interlocking occurs when the paint penetrates the irregularities such as holes, pores, and crevices on the surface, and is then mechanically locked to these surface features after hardening and paint curing.

Processes of mechanical roughening of the surface can be used in order to improve paint performance and reduce corrosion propagation. Sand blasting and grit blasting are the most commonly used in the Oil and Gas Industry. Although these methods fulfill the application requirements, they present disadvantages such as high energy usage, high supply costs, high operational costs, and high environmental impact (Schweitzer, 2007).

For the past decades, laser technology has been used in many industrial applications. Welding, additive manufacturing, communications, and sensors are a few examples among many. In addition, due to its surface modification capabilities, the laser material removal process can also be a viable technology for surface preparation. Laser surface modification is carried out by removing small amounts of material through laser ablation (Etsion, 2005). To achieve different surface conditions and topography, there are many laser parameters that can be controlled such as pulse energy, repetition rate, and wavelength, as well as process strategies such as scan speed and direction, pulse overlap, number of passes, etc. (Dubey and Yadava, 2008). Percussion laser drilling is one strategy that consists of firing consecutive pulses at one specific spot of the surface. It is commonly used for hole drilling with the main advantages of process speed and excellent control of shape and positioning of the textured structure. Preliminary experiments must be performed to understand the effect of processing parameters in relation to dimensional and geometrical characteristics of the machined holes.

This research work aims at understanding single pulse and multi pulse interactions as well as the response of varying laser parameters on the generated structure and their correlation to the laser damage threshold experiments. The laser damage threshold can be described as the limit of energy density (energy per area) over which a determined material can suffer laser ablation. This threshold can provide important information regarding the interaction between a laser beam and a specific material (Nath, 2014). Thus, the findings presented here will assist on the development of more complex structures in future research.

2. MATERIALS AND METODOLOGY

Samples with dimensions of 10 mm x 10 mm x 6 mm were prepared from AISI 1020 steel plate. The sample surface was ground with decreasing SiC grit size abrasive papers up to mesh # 1200 and polished down to a mirror-like surface finish.

Laser surface irradiation was performed with a nanosecond pulsed fiber laser (model SP-070P-A-EP-Z-B-Y, SPI LASER, UK) at the fundamental radiation wavelength of 1064 nm. The laser provided pulses with pulse energy up to 1.0 mJ with an average power of 70W. The pulse duration and the pulse repetition rate can be varied between 10 to 500 ns, and 1 - 1000 kHz, respectively. The laser beam is delivered by the optic system (collimator, focusing lens) inside the processing head. The beam position on the sample was controlled by a galvanometer scanner.

The laser beam was focused on the sample top surface. The laser focal position was changed in the vertical axis by moving an adjustable linear lens controlled by the processing software. This configuration allows changing the focal plane over the steel sample. The processing head and laser source were controlled by a computer. Figure 1 shows a scheme of the experimental setup. Ablation threshold and percussion drilling experiments were carried out in an ambient environment.

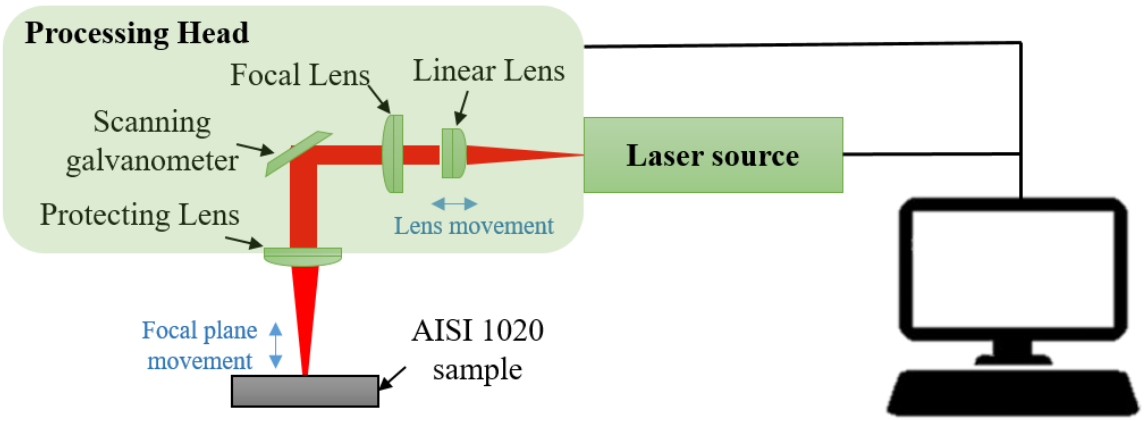

Figure 1. Schematic diagram of experimental setup.

2.1 Percussion drilling experiments

These experiments aim to understand the effects of the laser processing parameters on the hole geometry (diameter and depth). The response of varying laser parameters is examined through percussion drilling. The influence of pulse energy, number of pulses, and focal plane were evaluated. The related parameters are presented in Table 1.

Laser power was varied from 1 to 5.3 W. Pulse energy was increased in percentage values of 25%, 50%, 75%, and 100%. The related pulse energy values were 133 µJ, 266 µJ, 400 µJ, and 532 µJ. The number of pulses was varied between 5, 25, and 50 pulses. The pulse repetition rate was setup at 10 kHz. Three laser focal distance over the sample were evaluated, 0.0 mm, 1.0 mm, and 2.0 mm. At least 3 holes were fabricated for each experiment condition.

Table 1. Experimental parameters used in percussion drilling experiments.

Experimental parameters	**Values**
Pulse Energy, E_p (µJ)	133, 266, 400, 532.
Laser Power, (W)	1 – 5.3
Pulse duration time (FWHM), (ns)	46
Number of pulses per spot	5, 25, 50
Pulse repetition rate, (kHz)	10
Focal distance over the sample (mm)	0.0, 1.0, 2.0

The processed holes were examined using optical microscopy and scanning electron microscope (SEM). Holes' diameters and depth were characterized by optical microscopy using a ZEISS microscope model Axio Imager 2. The hole diameter was measured by a diameter evaluation tool on the microscopy image processing software (Axio Vision). The hole depth was measured by determining the focal position difference from the sample surface to the bottom of the hole, through the fine-focus knob of the microscope. The z accuracy of the fine-focus knob is 1 µm. At least 3 measurements of each condition were performed to determine holes' diameter and depth.

SEM images were used to evaluate the hole morphology after laser irradiation. SEM images were obtained by a Phenom ProX scanning electron microscopy.

2.2 Material ablation threshold experiments

The experiments aim to determine the single pulse ablation threshold for the AISI 1020 steel on different focal plane positions in relation to the sample top surface. For that, the average energy density was calculated using the equation (1):

$$\boldsymbol{F} = \frac{E_p}{\pi w_0^2}, \tag{1}$$

where Ep is the average laser pulse energy and ω_0 is the laser beam radius at e^{-2} of the Gaussian beam profile maximum intensity. The ω_0 value was estimated by the method described by Liu (1982), commonly known as the D^2-method. This method considers a laser beam with Gaussian energy distribution, thus, the fluence in a plane perpendicular to the laser beam can be estimated by the equation (2):

$$\boldsymbol{F(r)} = F_0 e^{\frac{-2r^2}{w_0^2}}, \tag{2}$$

where r is the distance to the spot center. The maximum fluence F_0 and E_p are related by equation (3):

$$\boldsymbol{F_0} = \frac{2E_p}{\pi w_0^2}, \tag{3}$$

Liu (1982) have demonstrated that for an ablation threshold fluence (F_{th}), the diameter (D) of an ablated crater is related to the peak fluence (F_0) by equation (4):

$$\boldsymbol{D^2} = 2\omega_0^2 ln(\frac{F_0}{F_{th}}), \tag{4}$$

Since F_0 increases linearly with E_p, the ω_0 value at the sample top surface can be estimated from the plot of the square of the average crater diameter (D^2) versus the logarithm of the pulse energy (ln E_p). Also, ω_0 is calculated from the slope obtained from a linear fitting to the experimental data. By extrapolation of D^2 back to zero, a value for the ablation threshold fluence can be obtained.

To obtain the experimental data, several craters were produced on the steel sample with increased pulsed energies. E_p was incremented by increasing the laser power. The experiments were performed with a pulse repetition rate of 10 kHz, and a pulse duration time of 46 ns. The irradiated craters were measured for a single pulse on the focal position. Table 2 presents the experimental parameters.

Table 2. Experimental parameters used in ablation threshold experiments.

Experimental parameters	**Values**
Pulse Energy, E_p (μJ)	50, 100, 200, 250, 350, 450, 532
Laser Power, (W)	1 – 5.3
Pulse duration time, (ns)	46
Pulse repetition rate, (kHz)	10
Focal position over the sample (mm)	0.0

The diameter of the irradiated craters was measured by optical microscopy using a ZEISS microscope. In order to avoid misleading measurements of crater diameters, the samples were chemically cleaned (Hydrochloric acid 40%, 5 seconds) to remove resolidified material near the crater. Figure 2 shows an optical microscope image of a crater before and after cleaning. At least 3 craters were evaluated for each test condition.

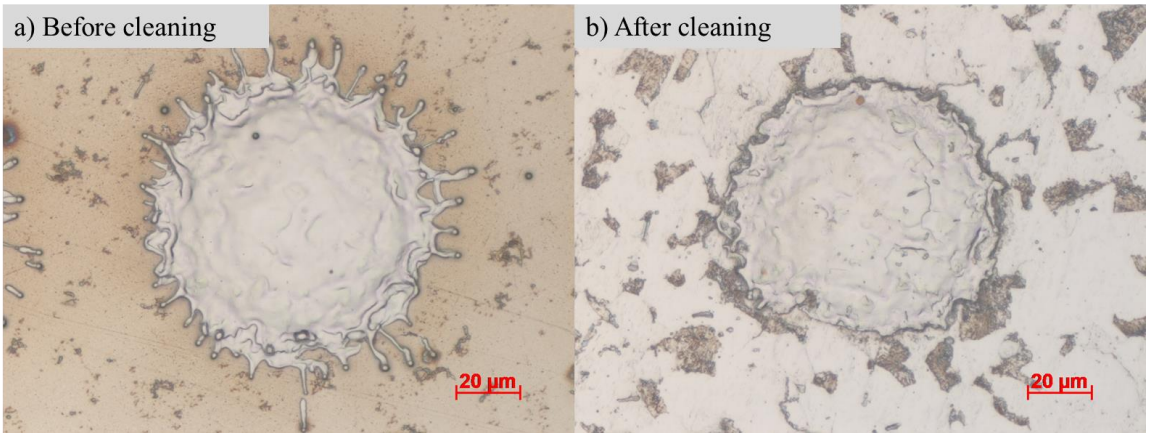

Figure 2. Irradiated craters a) before cleaning and b) after cleaning.

3. RESULTS

In this section, the results of percussion drilling and material ablation threshold experiments are presented separately.

3.1 Percussion drilling experiments

Percussion drilling holes fabricated on AISI 1020 steel with a 1064 nm wavelength Yb fiber pulsed laser were characterized. The effect of pulse energy, the number of pulses, and focal position over the sample were evaluated. Results of hole diameter and depth are presented in Figure 3.a and Figure 3.b, respectively. The chosen parameters affect the hole's dimensions in different manners. Results show different trends (indicated by the black arrows in Figure 3), which are explained separately in the following figures.

SEM images in Figure 4 show the effect of pulse energy on hole diameter of the percussion drilled holes. Focal position over the sample surface at 1 mm and 25 pulses per hole were kept constant. Results show that there is an incremental trend of increasing hole diameter values with the increase of pulse energy. In the laser material removal process, the surface absorbs the laser energy, which induces a local temperature increase. When the energy is above the ablation threshold (minimum energy necessary for material ablation) the material is melted and/or evaporated.

As the peak energy increased, the volume of the material above the ablation threshold increases, and therefore, the hole diameter increases (Ulerich *et. al.*, 2007). Figure 4 shows the presence of recast layer at the hole rim due to re-solidification of the ejected melted material from the hole. Also, it can be noticed that there is a significant increase in the amount of the solidified material with the increase of pulse energy. This is related to the larger amount of material removed.

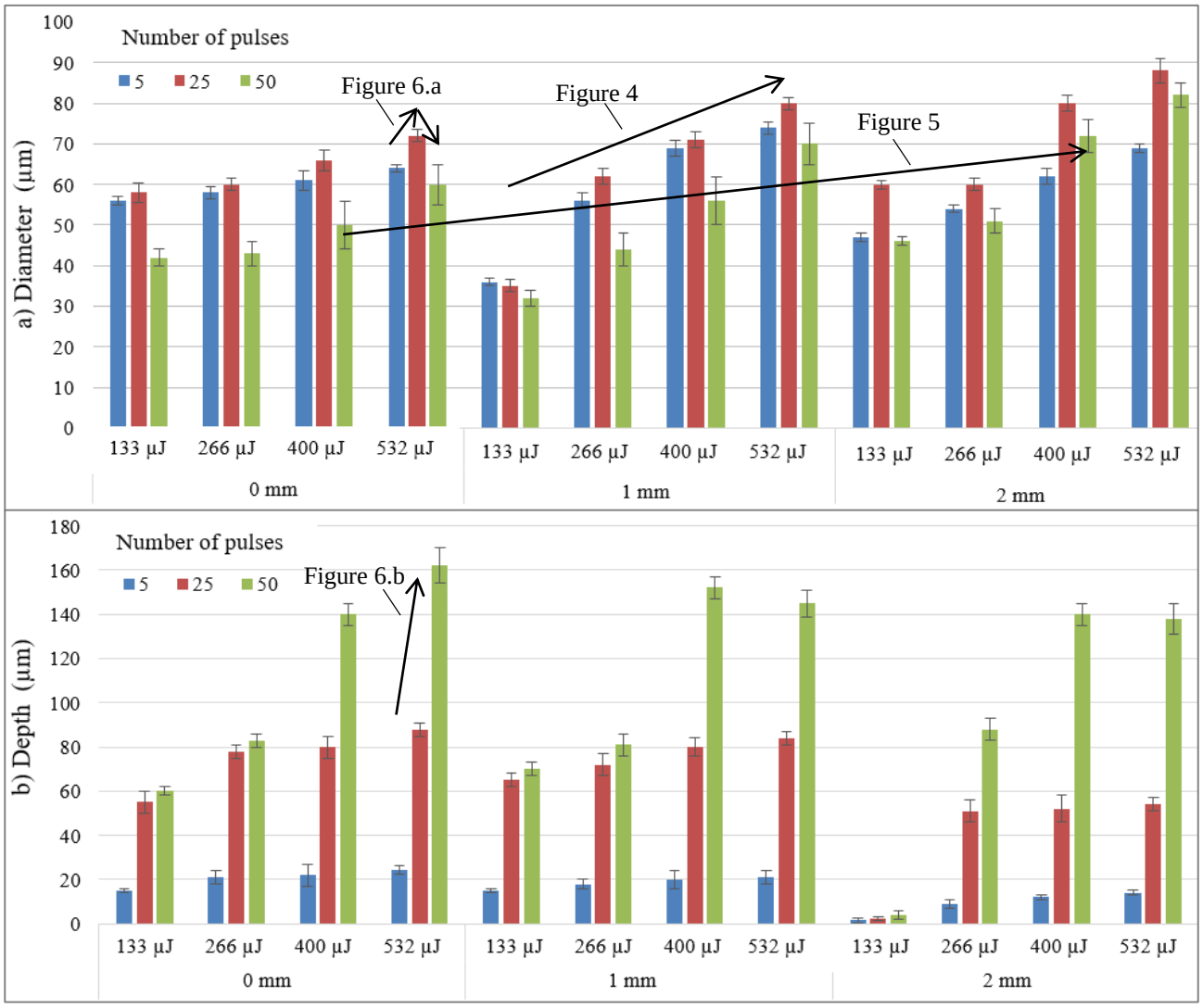

Figure 3. a) Diameter and b) Depth of laser irradiated holes as function of process parameters.

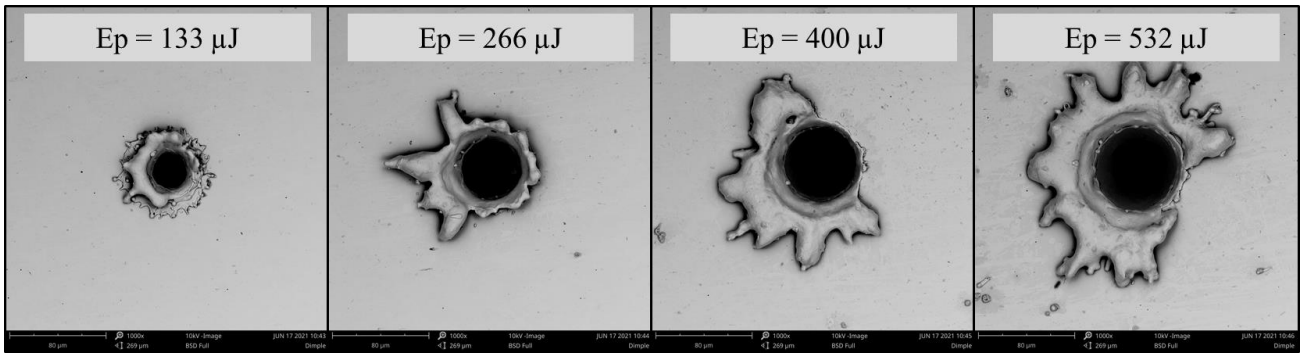

Figure 4. Effect of pulse energy on hole diameter. Focal distance is 1 mm over the sample surface; 25 pulses.

Experiments of percussion drilling with 50 pulses at a pulse energy of 400 µJ were performed with varying the focal distance over the sample surface. The effect of the increasing focal distance is presented in Figure 5. Results show an incremental trend of hole diameter with the increase of focal distance values over the sample top surface. The focal spot diameter at the sample surface, which determines the laser energy density is governed by the finite divergence of the laser beam, the laser beam energy distribution, and the optical lens characteristics (Nath, 2014).

By increasing the focal distance in relation to the sample top surface, there is an increase in beam-matter interaction surface area. However, the sample surface is irradiated with a lower energy density. For the tested conditions, it can be

seen that the material was ablated up to a distance from the center of the focal spot at different focal distances, as laser fluence was above the ablation threshold resulting in a larger hole diameter.

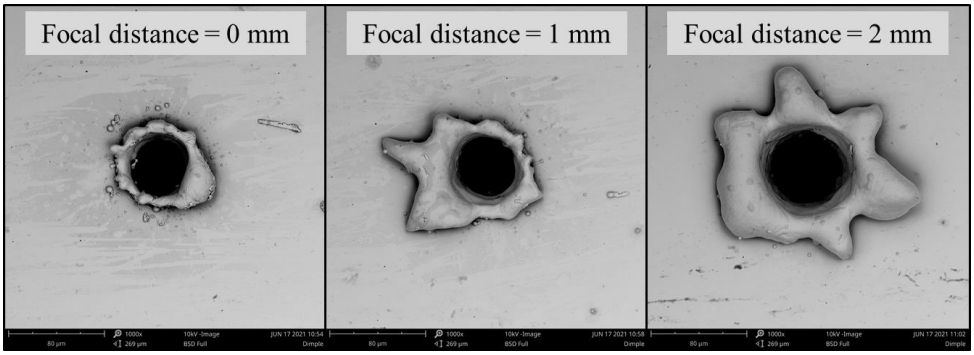

Figure 5. Effect of the focal distance over the sample on hole diameter. Energy was 400 µJ; 50 pulses.

Figure 6.a and Figure 6.b show the effect of the number of pulses on the hole diameter and the hole depth, respectively. It can be noticed in Figure 3 and Figure 6.a that the hole diameter slight increases when the number of pulses is increased from 5 to 25 pulses. On the other hand, an increase to 50 pulses results in smaller hole diameters. Figure 6.b shows that the hole depth increases with the applied number of pulses. In percussion drilling, a series of short-duration identical laser pulses is directed to the same spot. Each laser pulse removes material up to a certain depth, thus the hole depth increases with the number of pulses. The extend of the recast layer formed is found to vary with depth, and its thickness is particularly significant at the entrance side of the hole as compared to the middle and bottom side of the hole. Greater recast layer formation near the hole entry-side is caused by the molten material ejection. Figure 6.b shows a cross-sectional image of the holes produced with different number of pulses. It can be seen the formation of resolidified material at the entrance side of the hole, which generates the measured smaller hole diameters.

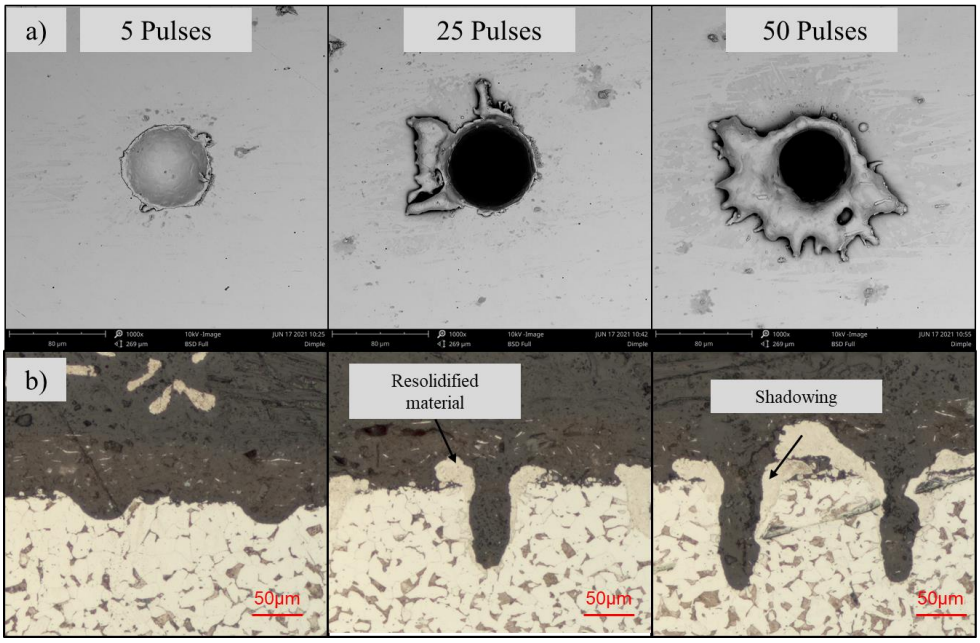

Figure 6. Effect of the number of pulses on a) hole diameter and b) hole depth. Energy was 532 µJ, focal position was on the sample surface.

It is important to notice that there is a penetration depth rate reduction with an increase of the number of pulses. This effect can be related to the recast layer formation in the keyhole evolution during percussion drilling (Zemaitis, 2018). The thickness of the layer consisting of liquid and resolidified material on the wall grows, yields to a closure of the hole by the melted material and therefore to shadowing of the laser irradiation. Also there is the tendency to form an equilibrium state in which, it is more difficult to expel the vaporized metal from the cavity (Ki. *et al.*, 2001). As a result, the hole depth increases at smaller rates, or even, saturates.

3.2 Material ablation threshold experiments

Results for the single pulse ablation threshold of the AISI 1020 steel on different focal plane positions over the sample are presented in this section. Figure 7 shows the laser-induced craters produced on the sample surface in stationary conditions, with average pulse energies from 50 µJ to 532 µJ. Craters' ablation using nanosecond laser is characterized by the predominance of melting and ejection of molten material. The micrograph images show an increased tendency of craters diameter with the increase of pulse energy. The ablation process starts when the target material absorbs the incident laser energy with a fluence level equal to or greater than the ablation threshold. As the peak energy is increased, the volume of the material above the ablation threshold increases, and as consequence the diameter of the irradiated crater increases.

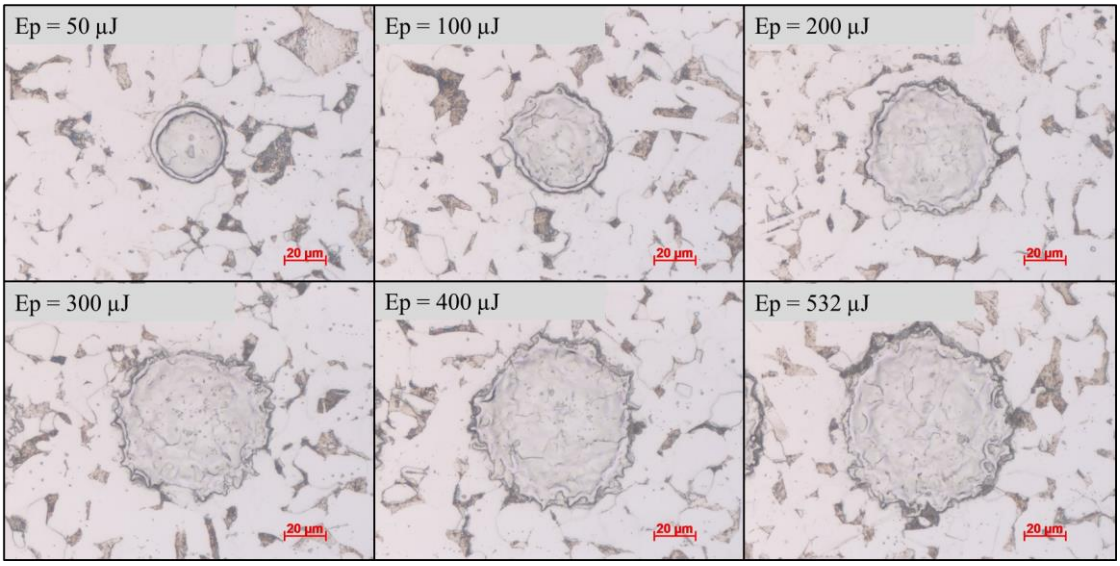

Figure 7. Laser-induced craters produced on AISI 1020 steel surface with average pulse energies in the range of 100 – 1000 µJ. Vertical position was 0 mm over the sample surface.

Figure 8 shows the square of the diameter of the ablated crater versus the natural logarithm of pulse energy. By extrapolation of D^2 back to zero, a value for the ablation threshold fluence was obtained. For the tested conditions, the measured ablation threshold for AISI 1020 steel was about 3.5 J/cm^2. Also, ω_0 was calculated from the slope obtained from the linear fitting by equation (4), and a value of 35.7 µm was obtained.

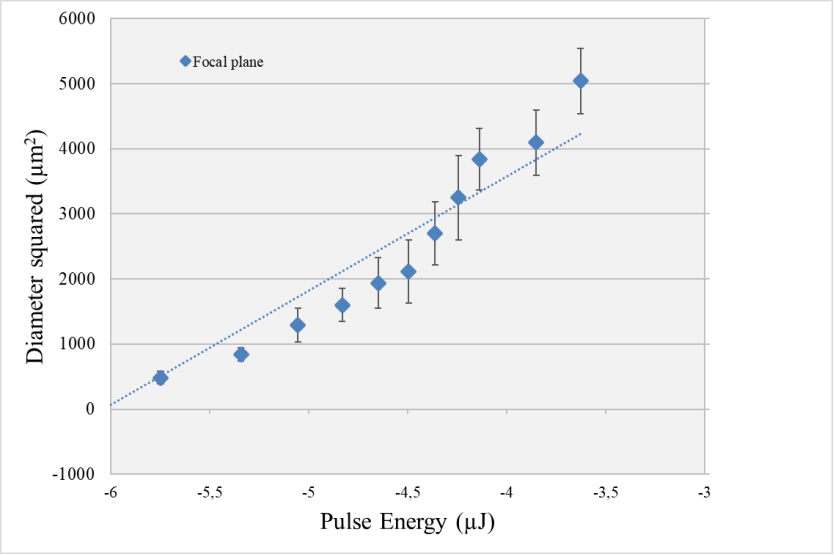

Figure 8. Relationship between D^2 and ln(Ep) under different pulse repetition rate with a single pulse.

4. CONCLUSION

The experiments carried out within the scope of this research have demonstrated a correlation between varying laser parameters and the holes dimensions on percussion drilling experiments. An increase in pulse energy and focal distance have both resulted in an increase in hole diameter. Increasing the number of pulses from 5 and 25 has also produced holes of bigger diameter, however, a higher amount of resolidified material has caused a decrease in measured diameter for 50 pulses. Regarding the hole depth, it has been found that increasing the number of pulses has the most significant effect on depth increase, whereas there is a much smaller relationship between the increase in pulse energy and an increase in depth. On the other hand, an increase in the focal distance has resulted in a slight decrease in the crater depth.

Moreover, with an increase in pulse energy and in the number of pulses, there is a greater amount of resolidified material as larger volumes of material are processed, which affects the shape and dimensions of the generated crater. Due to the complexities of the involved heat transfer and fluid dynamics mechanisms, there are many other variables that may impact the solidified material such as convection and pressure within the crater which were not considered in this research.

The results will aid the development of more complex structures in future studies such as grooves and grids, along with their effect on corrosion resistance of organic coatings applied over laser textured surfaces.

.

5. ACKNOWLEDGEMENTS

The authors gratefully acknowledge to the Instituto Senai de Inovação em Sistemas de Manufatura e Processamento a Laser and to Conselho Nacional de Desenvolvimento Científico e Tecnológico (CNPq) for the assistance provided for the development of this work.

6. REFERENCES

Dubey, A.K., and Yadava V. 2008. “Laser beam machining - A review”. *International Journal of Machine Tools and Manufacture.* Vol. 48, n. 6, pp. 609–28.

Etsion, I. 2007. “State of the Art in Laser Surface Texturing”. *Journal of Tribology.* Vol. 127, n.1, pp 248-53.

Hagen, C., Hognestad, A., Knudsen, O.Ø., Sørby, K. 2019. “The effect of surface roughness on corrosion resistance of machined and epoxy coated steel”. *Progress in Organic Coatings.* Vol. 130, pp. 17–23.

Ki, H., Mohanty, P. S., and Mazumder, J. 2001. “Multiple reflection and its influence on keyhole evolution”. *International Congress on Applications of Lasers & Electro-Optics.* Vol 2001, n. 1, pp. 933-942.

Liu, J.M. 1982. “Simple Technique for measurements of pulsed Gaussian-beam spot sizes”. *Optics Letters,* Vol. 7. pp. 196-198.

Nath, A.K., 2014. “Laser Drilling of Metallic and Nonmetallic Substrates”.

Papavinasam S. 2013. “Corrosion Control in the Oil and Gas Industry”

Schweitzer, P. 2007. “Fundamentals of Metallic Corrosion: Atmospheric and Media Corrosion of Metals”. *Journal of the American Chemical Society. Vol. 129, n. 15, pp. 4855–4855.*

Ulerich, J.P., Ionescu, L.P., Chen, J., Soboyejo, W.O., Arnold, C.B. 2007. “Modifications of Ti-6Al-4V Surfaces by Direct-Write Laser Machining of Linear Grooves”. *Photon Processing in Microelectronics and Photonics VI.* Vol. 6458, Internation Society for Optics and Photonics.

Žemaitis, A., Gaidys, M., Brikas, M., Gečys, P., Račiukaitis, G., & Gedvilas, M. 2018. “Advanced laser scanning for highly-efficient ablation and ultrafast surface structuring: experiment and model”. *Scientific reports,* Vol 8, n. 1, pp. 1-14.

7. RESPONSIBILITY NOTICE

The authors are the only responsible for the printed material included in this paper.